

The multi-mode Bessel-Gaussian beams OAM holographic method

XUFENG YUAN¹ AND CHAOYING ZHAO^{1,2,*}

¹College of Science, Hangzhou Dianzi University, Zhejiang 310018, China.

²State Key Laboratory of Quantum Optics and Quantum Optics Devices, Institute of Opto-Electronics, Shanxi University, Taiyuan 030006, China

*zchy49@163.com

Compiled May 8, 2024

In this paper, We prepare a multi-mode Bessel-Gaussian (MBG) selective hologram by stacking different mode combinations of Bessel-Gaussian phases on a multi-mode Bessel-Gaussian saved hologram in stages. Using a multi-mode BG beam with opposite combination parameters to illuminate the MBG-OAM hologram, the target image can be reconstructed after Fourier transform, and the sampling constant of this scheme is flexible and controllable. The encoding of holograms includes multiple BG mode combination parameters. When decoding incident light, the corresponding mode combination parameters must be met in order to reconstruct the image. This can effectively improve the security of OAM holography and the number of multiplexing channels. © 2024 Optica Publishing Group

Optica Publishing Group

<http://dx.doi.org/10.1364/ao.XX.XXXXXX>

1. INTRODUCTION

The holographic display technology invented by Gabor in 1948 is a technique that utilizes the principles of interference and diffraction of light to record the three-dimensional information of an object in the form of an interference pattern within a holographic medium and then reconstructs the three-dimensional object's light field wavefront through a laser beam [1]. Optical holography has been widely applied in recent years in areas such as three-dimensional displays [2–7], optical shaping [8], holographic multiplexing [9, 10], microscopic imaging [11], optical encryption [12], and information storage [13]. In these applications, optical holography achieves multi-channel, high-capacity systems through multiplexing in various optical dimensions such as Frequency division multiplexing [14], time division multiplexing [15], polarization [16], angle [17, 18], and frequency. However, the bandwidth of existing dimensions is limited. In 1992, Allen et al. experimentally demonstrated that each photon of a Laguerre-Gaussian beam (LGB) carries orbital angular momentum (OAM) [19] with a value of $l\hbar$, where l is known as the topological charge (TC) and represents the vortex beam's topological charge. The OAM can be represented by a spiral phase of $e^{il\varphi}$ where φ is the azimuthal angle. With further research, it has been shown that the topological charge can also

be a fraction [20]. Different topological charges represent different eigen-states, meaning that OAM has an infinite number of eigen-states that are orthogonal to each other. Therefore, utilizing OAM as a new degree of freedom for information processing can further enhance the bandwidth of optical communications.

However, due to the lack of OAM selectivity in traditional holographic design, OAM has not been realized as a holographic information carrier. In July 2019, Ren et al. proposed an OAM holography scheme [?], in which they used OAM as an independent information carrier for holographic information processing and demonstrated the multiplexing and demultiplexing processes of surface orbital angular momentum holography using a micro-hologram composed of GaN nano-pillars.

The high capacity and high resolution of OAM holography generally cannot be achieved at the same time. The larger the information capacity of the OAM hologram, the lower the resolution. To avoid cross-talk between the various OAM channels of the hologram, it is necessary to ensure that the OAM properties of each pixel position are not destroyed. This is generally done by sparsely sampling the original image. However, as the number of OAM modes increases, the sampling constant increases, resulting in severe loss of image resolution. This bottleneck problem greatly limits the improvement space for the capacity and resolution of OAM holography technology. However, since the sampling constant of the sampling matrix used in hologram production depends on the spatial frequency of the OAM beam, the number of samples of the original image decreases as the topological charge number of the OAM beam increases. When the number of samples is too small, the target image information cannot be distinguished. To reduce the impact of sampling constants, in 2024, Ji et al. proposed a Bessel-Gaussian orbital angular momentum holography (BG-OAM) scheme [21]. Based on the self-healing property of the Bessel-Gaussian (BG) beam during propagation and its Fourier transform, which is a perfect vortex mode (different OAM modes have fixed ring radii), the BG-OAM holography scheme can effectively reduce the limitations of different OAM modes on sampling constants, improve security, and enhance anti-interference performance.

The principle of the OAM holography scheme is based on the complementarity of OAM opposite angular quantum numbers and the special wavefront of OAM beams. Therefore, OAM beams with the same characteristics can be theoretically applied to OAM holography. In recent years, the generation and ap-

plication of multi-mode vortex light have been studied in Ref. [22, 23]. The application of multi-mode vortex light with various combined modes to holography schemes is expected to increase the number of holography multiplexing channels and improve the security of holography demodulation. Multi-mode vortex light is a superposition state of different OAM lights. The amplitude and phase of the OAM beam in the superposition state will be redistributed. The amplitude of the superposition state OAM beam generally shows petal-like or multi-ring shape, while the phase is the superposition result of the phases of each single-mode OAM light, which still follows the principle of complementarity of OAM opposite angular quantum numbers. Therefore, by changing the combined mode of the multi-mode vortex light, the superimposed phase can be changed to form encoded holograms with different decoding methods. So far, no scheme has been proposed to combine multi-mode vortex light with holography. In this paper, we propose a holographic method based on multi-mode Bessel-Gauss orbital angular momentum (MBG-OAM) and verify the correctness of the MBG-OAM scheme through numerical simulation. Firstly, the MBG-preserving hologram is generated using computer-generated holography, and the phase of single-mode Bessel-Gauss beams with specific cone parameters a and angular quantum numbers l is superimposed to create the MBG selection hologram. When reconstructing the target image, an MBG beam with opposite selective holographic parameters (a, l) to the specific MBG beam is used to illuminate the MBG-OAM selection hologram, and the target image can be reconstructed after Fourier transformation.

The designed scheme utilizes the adjustable ring radius of the BG beam to achieve OAM selective holography without destroying the OAM characteristics in higher topological cases, realizing flexible and controllable sampling constants. The encoded phase of the hologram contains multiple selective holographic parameters (a_n, l_n) combinations, and the incident light during decoding must satisfy the superimposed state MBG beam with ($-a_n, -l_n$) parameter combinations to reconstruct the image. In addition, the maximum multiplexing channel count of previous OAM holography is generally equal to the number of available OAM modes, but in this scheme, the additional coding degree of freedom provided by combining the BG beam with multi-mode OAM offers more multiplexing channels and higher security for holography. In practice, the number of multiplexing channels is affected by the performance of the actual OAM light and spatial light modulator.

2. PRINCIPLES AND METHODS

The working principle of our proposed multi-mode Bessel Gaussian beam orbital angular momentum (MBG-OAM) holographic scheme is shown in the figure As the light source, the laser beam

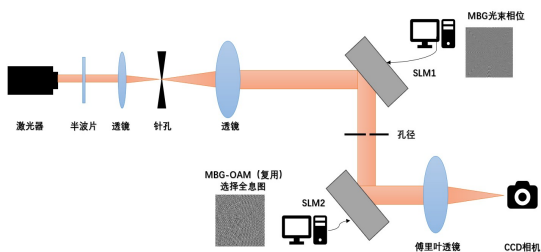


Fig. 1. MBG-OAM Holographic scheme

is modulated into polarized light parallel to the working direction of the first spatial light modulator (SLM) after passing through a half wave plate, shaping and expanding through a lens group and pinholes. SLM1 is loaded with the phase of a multi-mode BG beam, so the incident polarized light can be modulated into a specific MBG beam. After being limited by the aperture (only diffraction level light of $+1$ or -1 can pass through), it is incident onto SLM2 loaded with MBG-OAM selected holograms or MBG-OAM multiplexed holograms. After passing through the Fourier lens, it is incident onto the sensor (charge coupled, CCD) on the rear focal plane. On. The Gaussian point image of the target image can only be reconstructed when the phase of the MBG on SLM1 is opposite to that on SLM2.

A. Bessel-Gaussian beams and multi-mode vortex beams

In cylindrical coordinates, Bessel Gaussian beam as an approximation of Bessel beam can be expressed by [24]

$$E_{BG}(r, \varphi, z) = J_l(k_r r) e^{il\varphi} e^{ik_z z} e^{-\frac{r^2}{w_0^2}} \quad (1)$$

here, w_0 is Gaussian beam waist radius, $k_z = k \cos \theta$, $k_r = k \sin \theta$, $k = 2\pi/\lambda$ are propagation direction wave-number, radial wave-number, and wave-number, respectively, $J_l(k_r r)$ is the first type of l -order Bessel functions

$$J_l(k_r r) = \sum_{m=0}^{\infty} \frac{(-1)^m}{m! \Gamma(m+l+1)} \left(\frac{k_r r}{2}\right)^{2m+l} \quad (2)$$

here, $\Gamma(x)$ is gamma function, when x is a positive integer

$$\Gamma(x) = (x-1)! \quad (3)$$

BG beams can be generated using SLM loaded phase masks instead of axi-prisms to generate [25]. The phase mask function is $e^{il\varphi + iar}$, where a and l are the parameters of the axi-prisms and the topological charge of the BG beam, respectively. After the Gaussian beam is incident on SLM, a BG beam with radial and longitudinal components can be formed. Adjusting a and l can effectively control the ring radius of the generated BG vortex beam. After passing through the Fourier lens, the BG beam becomes a Perfect Optical Vortex (POV), and the unique radius characteristics of the POV make the BG-OAM holographic beam. The scheme greatly reduces the limitation of sampling constants on holograms in high-order modes. When reconstructing images using computational holography, a single mode BG-OAM hologram without incident light undergoes a Fourier transform to obtain the target image constructed by a perfect vortex light mode.

Multi-mode vortex light refers to a beam of light containing different modes of orbital angular momentum. Single mode vortex light has a hollow annular light field distribution. When a light beam is in the superposition state of multiple mode orbital angular momentum beams, the light field distribution of its cross section is petal shaped due to the superposition of different OAM modes, and its phase distribution is also different from that of a single mode. For example, when two vortex beams with topological charges of l_1 and l_2 are coaxial beams of equal intensity, their complex amplitudes can be expressed as

$$E \propto e^{il_1\varphi} + e^{il_2\varphi} \quad (4)$$

From this, the corresponding light intensity distribution can be obtained

$$|E|^2 \propto \left| e^{il_1\varphi} + e^{il_2\varphi} \right|^2 = 2 \{1 + \cos[(l_1 - l_2)\varphi]\} \quad (5)$$

Figure 1 show that the cross-sectional intensity distribution and phase distribution of different l_1 and l_2 proportional dual-mode mixed vortex beams at the waist of the beam are listed. When

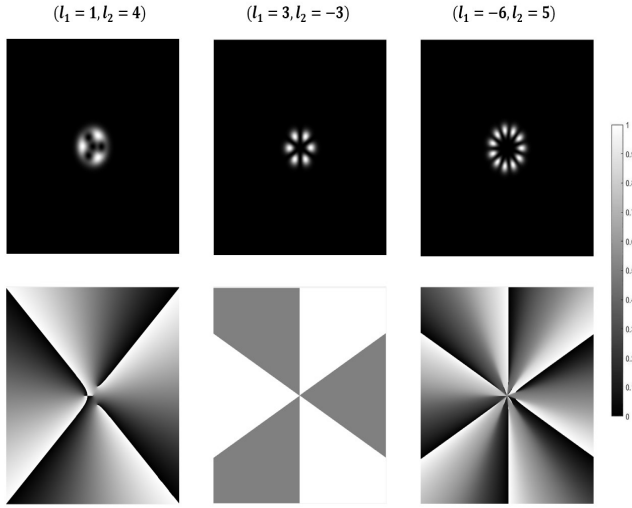


Fig. 2. Cross section intensity distribution and phase distribution of different proportional dual-mode mixed vortex beams of l_1 and l_2 at the waist of the beam

the number of modes involved in stacking increases or the proportions of each mode are different, the cross-sectional light intensity distribution and phase distribution become more complex. In summary, the multi-mode vortex light composed of BG beams can be represented as:

$$E \propto e^{il_1\varphi+ia_1r} + e^{il_2\varphi+ia_2r} + \dots + e^{il_n\varphi+ia_nr} \quad (6)$$

Due to the adjustable ring radius of single-mode BG beams, the radius of MBG beams is affected by the radii of each single-mode BG beam participating in the superposition.

B. multi-mode Bessel-Gaussian beam OAM holographic scheme

Previously, holograms generated by traditional computer holography had a continuous spatial frequency distribution and could not preserve the circular features of the OAM beam. Therefore, to achieve OAM holography, it is necessary to sample the original image while preserving the effective information of the original image, so that each sampling point in the hologram can effectively preserve the spiral wavefront of the OAM beam. According to the opposite OAM cancellation principle, OAM selective holography and multiplexed holography can be achieved.

According to the Fourier transform property [26], the complex amplitude distribution of a beam is the spectral function of a spatial function

$$G(x, y) = \iint g(u, v) e^{-i2\pi(ux+vy)} dudv \quad (7)$$

In holography, $G(x, y)$ and $g(u, v)$ can represent the spatial function of the holographic plane and the spectral function of the image plane, respectively. (x, y) and (u, v) are orthogonal coordinates. In computational holography, the hologram is digitized,

so discretizing the spatial function yields the computational hologram

$$G(x, y) = \sum_{u=1}^M \sum_{v=1}^N g(u, v) e^{i2\pi(ux+vy)} \quad (8)$$

In order to achieve OAM selective holography, it is necessary to sample the image information with continuous spatial frequency distribution reasonably to avoid wavefront overlap causing damage to OAM characteristics. The original image is sampled using a two-dimensional Dirac comb function related to the OAM spatial frequency. The sampling constant d of the comb function is determined by the OAM spatial frequency. As the OAM beam used in this scheme is an MBG beam, the influence of the sampling constant on OAM holography can be reduced by adjusting the ring radius of the BG beam.

Using the two-dimensional Dirac comb function $Comb(x, y)$ to sample the original image $U(x, y)$ to obtain the target image $D(x, y)$, this process is described as

$$D(x, y) = Comb(x, y) \cdot U(x, y) \quad (9)$$

The two-dimensional Dirac comb function can be described as

$$Comb(x, y) = \sum_m \sum_n \delta[(x - mT_1)(y - nT_2)] \quad (10)$$

(x, y) is the Cartesian coordinates of the original image, T_1, T_2 are the sampling constants of the x, y axes, where $T_1 = T_2 = d$, m, n are the ordinal numbers of the sampling points on the x, y axes, respectively. Subsequently, a random phase P_r is superimposed on the sampled image and iterated using the Gerchberg Saxton(GS) algorithm [27]. After reaching the preset number of iterations, the OAM saved hologram is obtained. Overlay l -order BG beam phase with an axial prism parameter of a on the OAM saved hologram, so that the Fourier transform of the spiral wavefront is copied to each pixel of the hologram. This process can be expressed as

$$D_{BG}(x, y) = \mathcal{F}^{-1}[D(x, y) \cdot e^{-2\pi i \cdot P_r}] \cdot e^{il\varphi+iar} \quad (11)$$

\mathcal{F}^{-1} represents the inverse Fourier transform.

BG beam orbital angular momentum K-path multiplexing holography can be described as

$$D_{K-BG}(x, y) = \sum_{k=1}^K \mathcal{F}^{-1}[D_{k-BG}(x, y) \cdot e^{-2\pi i \cdot P_r}] \cdot e^{ik\varphi} \quad (12)$$

When the phase of the superimposed beam changes to the phase of the MBG beam, the above two equations can be corrected as follows

$$\begin{aligned} D_{MBG}(x, y) &= \mathcal{F}^{-1}[D(x, y) \cdot e^{2\pi i \cdot P_r}] \cdot (e^{il_1\varphi+ia_1r} + e^{il_2\varphi+ia_2r} + \dots + e^{il_s\varphi+ia_sr}) \\ &= \mathcal{F}^{-1}[D(x, y) \cdot e^{2\pi i \cdot P_r}] \cdot \sum_{s=1}^S e^{il_s\varphi+ia_sr} \end{aligned} \quad (13)$$

Among them, l_s and a_s are the topological charge and axial prism parameters of the s -th single-mode BG beam in the MBG beam, respectively, and S is the number of single-mode BG beams participating in superposition in the MBG beam. The MBG-OAM multiplexing hologram can be represented as

$$D_{K-MBG}(x, y) = \sum_{k=1}^K D_{k-MBG}(x, y) \quad (14)$$

$D_{k-MBG}(x, y)$ represents the k -th MBG-OAM hologram used for multiplexing.

Figure 3 show the design process of MBG-OAM saving holograms, MBG-OAM selecting holograms, and MBG-OAM multiplexing holograms.

When reconstructing the target image for the multiplexed hologram of Eq.14, based on the characteristic of restoring Gaussian mode through opposite topological charge cancellation, the topological charge of the incident MBG beam and the combination parameter $(a_1, l_1; a_2, l_2; \dots)$ of the prism parameter and the k -th MBG-OAM hologram are all opposite. That is, when the condition $(-a_1, -l_1; -a_2, -l_2; \dots)$ is met, the information carried by the k -th hologram can be reproduced, while other MBG modes cannot recover Gaussian mode. After filtering with a comb function array, the information carried by other phase modes can only be reproduced. The principle of not displaying information is described as follows

$$\begin{aligned} D_{rec}(x, y) &= \mathcal{F}[D_{K-MBG}(x, y) \cdot (-MBG_k)] \cdot Comb(x, y) \\ &= D_{k-MBG}(x, y) \end{aligned} \quad (15)$$

where $D_{rec}(x, y)$ represents the complex amplitude of the reconstructed image plane, \mathcal{F} represents the spatial Fourier transform, and $-MBG_k$ represents the MBG with completely opposite combination parameters to the k -th MBG beam. In this way, when using MBG light with different specific combination parameters for incident multiplexing holograms, different holographic images can be reconstructed.

3. SIMULATION AND ANALYSIS

Based on the computational holography method for target image reconstruction, the single-mode BG-OAM selected hologram without incident light is transformed by Fourier transform to convert the BG beam at each sampling point position into POV. As shown in the figure

A. Multi-mode Bessel-Gaussian beam OAM holography

To verify the feasibility of the MBG-OAM holographic scheme, we conducted simulation verification based on dual-mode BG light, and the entire process was implemented using computational holography. The encoding parameters of the MBG loaded on SLM2 mainly include the axial prism parameters, topological charges, and number of modes of the BG beams involved in stacking. For convenience in description, we use $(a_1, l_1; a_2, l_2; \dots)$ to describe a specific MBG beam. When reconstructing an image, theoretically, the combination parameters of the incident MBG light must satisfy $(-a_1, -l_1; -a_2, -l_2; \dots)$ before the image can be reconstructed.

Firstly, the original image "A" is sampled to obtain the corresponding MBG-OAM saved hologram, which is then overlaid with a dual-mode BG beam of $(-0.06, -3; -0.08, -2)$ to obtain the MBG-OAM selected hologram. When the incident light parameters are $(0.06, 3; 0.08, 2)$, $(0.06, 3; 0.08, 4)$, and $(0.06, 3; 0.1, 2)$, respectively, the MBG-OAM selects hologram can be obtained as shown in Fig.5.

The simulation results show that only MBG beams with $(0.06, 3; 0.08, 2)$ can reconstruct the target image "A" when illuminating the hologram, while MBG beams with other combination parameters can choose the hologram when illuminating MBG-OAM. The filtered image appears as a circular or irregular intensity distribution, which is the superposition result of MBG beams without mutually cancelling topological charges or prism parameters. When the topological charges cancel each

other out, the MBG beam with the $(0.06, 3; 0.1, 2)$ combination parameter illuminates the hologram, and after filtering, there is image information with lower brightness. This indicates that a can't be used as an absolute key decoding parameter. This is because the phase of the light field is redistributed after the BG beams with different ring widths are stacked, and the intensity distribution may illuminate the original center. The quality of the reconstructed image is still affected by a . Therefore, it is recommended that the MBG beam used for image reconstruction be consistent with the $|a|$ of the participating BG beams.

B. Multi-mode Bessel-Gaussian beam OAM multiplexing holography

When using MBG-OAM selection holograms for multiplexing holography, the degrees of freedom in multi-mode BG beams, such as topological charge, axial prism parameters, and the number of BG beams participating in superposition, are different. The MBG-OAM selection holograms generated by different combinations can carry different information, and the number of reuse channels breaks the previous limitation of only topological charge. More encoding degrees of freedom greatly improve the number of multiplexing channels and decoding security. To verify the feasibility of the MBG-OAM holographic multiplexing scheme, we conducted simulation verification based on dual channel MBG-OAM holography. Firstly, the original image "A" is sampled to obtain the corresponding MBG-OAM saved hologram, which is then overlaid with a dual-mode BG beam with a combination parameter of $(-0.06, -3; -0.08, -2)$ to obtain the MBG-OAM selected hologram 1. Sample the original image "B" to obtain the corresponding MBG-OAM saved hologram, and overlay it with a dual-mode BG beam with a combination parameter of $(-0.1, -5; -0.12, -1)$ to obtain MBG-OAM selected hologram 2. Overlay MBG-OAM selected hologram 1 and MBG-OAM selected hologram 2 to create an MBG-OAM multiplexed hologram, with overlapping positions of the two target images in the hologram. According to the variable method, MBG optical incident multiplexing holograms were tested and simulated by changing the topological charge, the topological charge, and the parameters of the prism, and only the parameters of the prism. As follows, when the parameters of the incident MBG light combination are $(0.06, 3; 0.08, 2)$, $(0.06, 3; 0.12, 1)$, and $(0.1, 5; 0.12, 1)$, the MBG-OAM multiplexed hologram is irradiated to obtain in Fig.5.

Figure 6 shows that the corresponding target image "A" and target image "B" can only be reconstructed when the combination parameters of the incident MBG beam are $(0.06, 3; 0.08, 2)$ and $(0.1, 5; 0.12, 1)$, respectively. Otherwise, due to the decoding parameter $(0.06, 3; 0.12, 1)$ and the combination parameters $(-0.1, -5; -0.12, -1)$ or $(-0.06, -3; -0.08, -2)$ not canceling each other, the reconstruction fails. The results indicate that the MBG-OAM holographic multiplexing scheme is feasible.

4. CONCLUSION

To improve the limitation of the number of channels for single-mode holographic multiplexing, based on the principle of multi-mode vortex beam superposition state and opposite OAM cancellation to recover Gaussian mode, combined with orbital angular momentum holography, we propose a new scheme: to produce multi-mode Bessel Gaussian selective holograms and multiplexed holograms by sequentially stacking different parameter combinations of Bessel Gaussian phase on multi-mode Bessel Gaussian saved holograms. Using MBG beams with completely

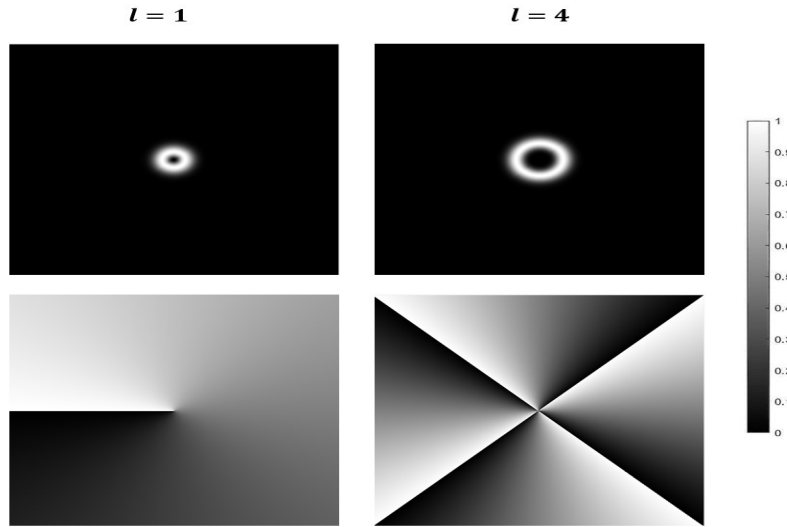


Fig. 3. (a)Original image, (b)sampling array, (c)MBG-OAM saved hologram, (d)multi-mode BG beam phase, (e)MBG-OAM selected hologram, (f)MBG-OAM multiplexed hologram.

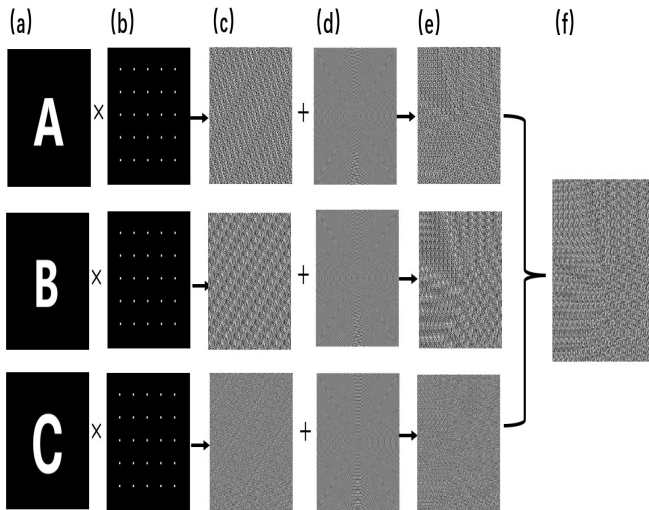


Fig. 4. Image reconstruction of BG-OAM selective holograms without incident light

opposite parameter combinations to illuminate MBG-OAM holograms, the target image can be reconstructed through Fourier transform. This scheme retains the advantages of BG-OAM holography, with flexible and controllable sampling constants, and increases the encoding freedom of the hologram. When decoding the incident light, the corresponding mode combination parameters must be met simultaneously to reconstruct the image, effectively improving the security of OAM holography and the number of multiplexing channels, which has high practical value.

Acknowledgments. Financial support from the project funded by the State Key Laboratory of Quantum Optics and Quantum Optics Devices, Shanxi University, Shanxi, China (Grants No.KF202004 and No.KF202205).

Disclosures. The authors declare no conflicts of interest.

REFERENCES

- Gabor and D, Proc. IEEE (1972).
- Huang and S. T., Proc. IEEE (1971).
- B. R. Brown and A. W. Lohmann, Appl. Opt. **5**, 967 (1966).
- C. Slinger, C. Cameron, and M. Stanley, Computer **38**, 46 (2005).
- T. C. Poon, *Digital Holography and Three-Dimensional Display* (Digital Holography and Three-Dimensional Display, 2006).
- W. Osten, A. Faridian, P. Gao, *et al.*, Appl. Opt. **53**, 44 (2014).
- E. Sahin, E. Stoykova, J. Mkinen, and A. Gotchev, ACM Comput. Surv. **53**, 1 (2020).
- L. Jin, H. Li, C. Zhao, and W. Gao, J. Opt. Soc. Am. A **36**, 1215 (2019).
- C. RosalesGuzmán, A. Trichili, A. Dudley, *et al.*, "Optical communications beyond orbital angular momentum," in *Spie Optical Engineering and Applications*, (2016).
- R. Zhao, L. Huang, and Y. Wang, PhotonIX **1** (2020).
- E. Lam, "Computational imaging and reconstruction in digital holographic microscopy," in *SPIE Structured Light Conference*, (2018).
- Uota and Kaoru, Opt. Eng. **43**, 2228 (2004).
- E. G. Ramberg, "Holographic information storage," (1972).
- T. Tahara, Y. Takahashi, and Y. Arai, J. Jpn. Soc. for Precis. Eng. **84**, 85 (2018).
- Z.Zhuqing, F. Shaotong, N. Shouping, and Z. Jiajie, Hologr. diffractive optics, applications IV (2010).
- Z. Zhuqing, F. Shaotong, N. Shouping, and Z. Jiajie, "Multi-image hiding method based on polarization multiplexing digital holography," in *Holography, diffractive optics, and applications IV*, (2010).
- R. Zhao, B. Sain, Q. Wei, *et al.*, Light. Sci. Appl. **7**, 95 (2018).
- L.Allen, M.W.Beijersbergen, R.G.C.Spreeuw, and J.P.Woerdman, Phys. Rev. A **45**, 8185 (1992).
- Y. Y. Li, H. Liu, Z. Y. Chen, and P. B. L. Yao, Opt. Rev. (2011).
- H. Ren, G. Briere, X. Fang, and et.al, Nat. communications **10**, 2986 (2019).
- J. Ji, Z. Zheng, J. Zhu, *et al.*, Chin. Phys. B **33**, 014204 (2024).
- Q. Li, C. Wu, X. Liu, *et al.*, Ann. der Physik **531**, 1900367 (2019).
- W. Ran, J. Chen, and G. Fu, Acta Opt. Sinica **42**, 0426001 (2022).
- G. Wu, F. Wang, and Y. Cai, Phys. Rev. A **89**, 043807 (2014).
- H. Zhou and T. Gen, Opt. Instruments **45**, 47 (2023).
- H. Chand, Sukhender, D. Joseph, *et al.*, "Fourier transform- an important tool for optics," in *Foundation of Computer Science (FCS)*, (2012).
- P. Memmolo, L. Miccio, F. Merola, *et al.*, Opt. Lasers Eng. **52**, 206 (2014).

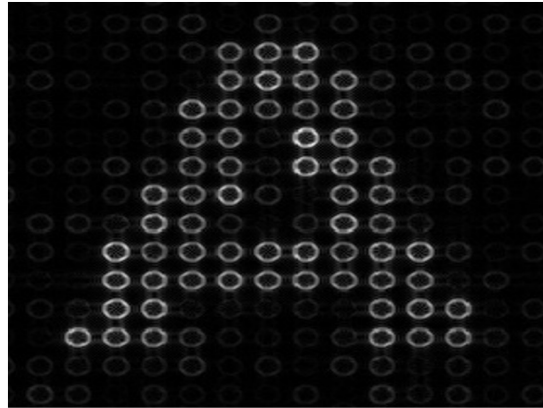


Fig. 5. MBG-OAM selects hologram image reconstruction: (a) target image, (b) MBG-OAM selects hologram and parameter combination, (c) combination parameters of incident MBG beam, (d) unfiltered reconstructed image, (e) details, (f) filtered image.

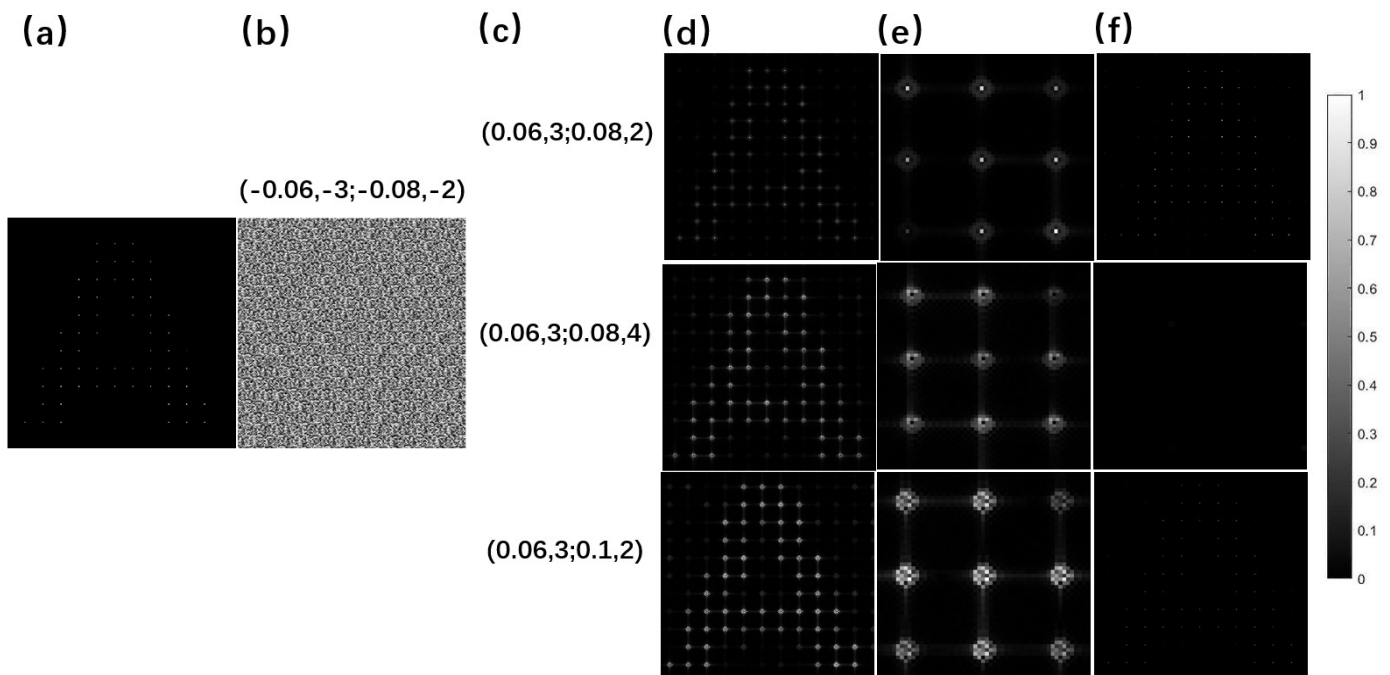


Fig. 6. Image reconstruction of MBG-OAM dual channel multiplexing hologram: (a) target image, (b) MBG-OAM multiplexing hologram and parameter combination, (c) combination parameters of incident MBG beam, (d) unfiltered reconstructed image, (e) details, (f) filtered image.